

## 29. GEOCHEMISTRY OF SEDIMENTS AT SITES 579, 580, AND 581, DEEP SEA DRILLING PROJECT LEG 86, WESTERN NORTH PACIFIC<sup>1</sup>

G. Ross Heath, Richard B. Kovar, and Carlos Lopez, Oregon State University<sup>2</sup>

### ABSTRACT

The elemental composition of sediments from Sites 579 ( $38^{\circ}38'N$ ,  $153^{\circ}50'E$ ) and 580 ( $41^{\circ}37'N$ ,  $153^{\circ}59'E$ ) is dominated by contributions from terrigenous detritus (including numerous thin ash beds) and opal-rich biogenic debris, with the terrigenous component increasing in dominance in the youngest sediments as the flux of Pleistocene eolian debris associated with Northern Hemisphere glaciation has increased. Diagenesis related to redox-sensitive reactions in near-surface sediments has had a marked impact on the distributions of Mn and S.

At Site 581 ( $43^{\circ}56'N$ ,  $159^{\circ}48'E$ ), the reduced biosiliceous clays corresponding to the sections at Sites 579 and 580 are underlain by a normal oxidized North Pacific "red clay" sequence. As at other North Pacific sites, the concentrations of Mn and Fe (as oxyhydroxides), Ba (as barite), and P (as fish debris) vary inversely with the accumulation rates of the clays. The cherts underlying the clays at Site 581 are noteworthy for their high P contents (comparable to values for biosiliceous clays) and high Fe and Mn relative to Ti and Al, suggestive of derivation from well-oxidized pelagic sediments.

### INTRODUCTION

#### Setting

During Deep Sea Drilling Project (DSDP) Leg 86, holes were drilled in pure calcareous ooze (Site 577), pelagic "red" clay (Site 576), and carbonate-free pelagic clay with variable contents of biogenic silica and volcanic ash (Sites 578–581). This chapter focuses on the elemental composition of sediments from Sites 579 ( $38^{\circ}38'N$ ,  $153^{\circ}50'E$ ), 580 ( $41^{\circ}37'N$ ,  $153^{\circ}59'E$ ), and 581 ( $43^{\circ}56'N$ ,  $159^{\circ}48'E$ ) (Fig. 1) in order to assess the roles of temporally varying biogenic and ash inputs and of *in situ* redox conditions in establishing the geochemical character of such deposits. The soft sediments at Sites 579 and 580 were cored continuously by hydraulic piston corer. The more indurated Site 581 sediments were recovered by conventional wire-line rotary coring. Because the upper section (0–181.5 m sub-bottom) of Hole 581 was not sampled, we report only on deeper portions of the section at this site.

The descriptions of the sediments at Sites 579 and 580 (see Site 579 and 580 chapters, this volume) show them to be uniform gray and greenish gray siliceous clay and siliceous ooze that accumulated at rates of about 35 and 50 m/m.y., respectively, interrupted by 61 (Site 579) and 89 (Site 580) identifiable ash beds and numerous dark greenish gray indurated layers that may be altered basic ash layers. Our samples, taken approximately 1.5 m apart, were placed so as to avoid both ashes and indurated layers. The color of the sediment and the presence of fine pyrite grains point to strongly reduced conditions ( $\text{Fe}^{3+}$  and  $\text{SO}_4^{2-}$  reduction) throughout both sections.

The section from 0 to 224 m at Site 581 (0–9 m.y. ago) is assumed to resemble the sections at Sites 579 and 580, although only the interval below 181 m (with an accumulation rate decreasing downcore from ~12 to ~4 m/m.y.) was cored continuously. From 224 to 245 m (9 to ~14 m/m.y. ago), the sediments are brown and light brown pelagic clays (that accumulated at about 4 m/m.y.), with small but variable concentrations of biogenic silica that decrease downcore and are rare at the base of the interval. The deepest clays (245–276 m) are very dark brown "slick" pelagic deposits typical of early to middle Tertiary deposits from vast areas of the North Pacific. Below 276 m, only small fragments of porcellaneous chert were recovered. From the behavior of the drill, the chert is believed to form thin beds in pelagic clay. The intense circulation of seawater required to keep chert fragments away from the bit washed away all the soft sediment, however.

#### Methodology

Samples were freeze-dried, disaggregated by shaking with methacrylate spheres in polycarbonate sample tubes, pressed into pellets, and analyzed by X-ray fluorescence using a Phillips PW-1600 simultaneous spectrometer. Raw counts for each element were ratioed to U.S. Geological Survey (USGS) standard SY3, which was run before and after each sample, and then converted to concentrations using a fundamental parameters program (Criss et al., 1978). Analyses of standard rocks and sediments indicate no systematic errors for the elements discussed. Analytical precision (counting statistics) is better than 2% for the elements reported, but sample to sample variability at the same level in a core is closer to 5% of the reported concentrations.

In order to determine the number of components in the Leg 86 sediments, we analyzed the elemental data using Q-mode factor analysis (Klovan and Imbrie, 1971). The empirical orthogonal functions (factors) generated

<sup>1</sup> Heath, G. R., Burckle, L. H., et al., *Init. Repts. DSDP*, 86: Washington (U.S. Govt. Printing Office).

<sup>2</sup> Address: (Heath, present address) College of Ocean and Fishery Sciences, University of Washington, Seattle, WA 98195; (Kovar, Lopez) College of Oceanography, Oregon State University, Corvallis, OR 97331.

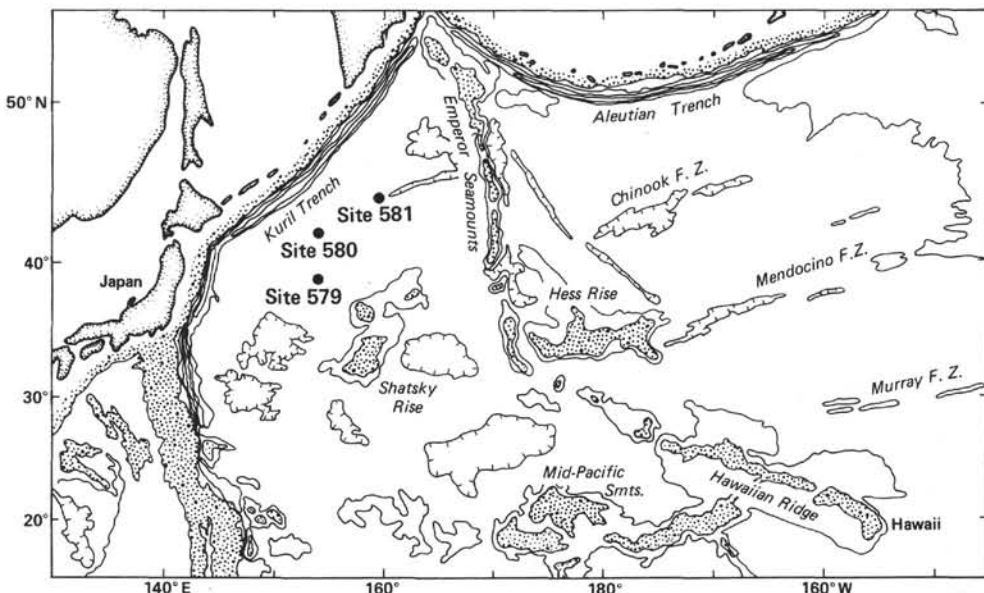


Figure 1. Location of Sites 579, 580, and 581 relative to major physiographic features of the western North Pacific (after Chase, 1975). Areas shallower than 4 km stippled; 5-km contour plain; 6-km contour hatched.

by this technique distribute the variance in the raw data as equally as possible between a subjectively selected number of "factors." We chose three factors in all of our analyses because this number accounted for 97% or more of the variance in the data sets.

## RESULTS

The major-element analytical results for Sites 579, 580, and 581 are summarized in Tables 1 to 3. Figures 2 to 4 show downhole plots of elemental abundances that illustrate the major compositional variations at the three sites.

Titanium, which is typical of elements supplied in detritus, shows similar distributions in the sections at Sites 579 and 580 (Fig. 2). For the past 1 m.y., values have been relatively high (0.36 and 0.35%, respectively), with standard deviations of 8 to 10%. Concentrations decrease downhole by about a third in the deposits older than 2 m.y., apparently due to dilution of the terrigenous component by biogenic opal. At the base of Hole 579, which is older than the base of Hole 580, Ti and several other elements (Fig. 2) increase slightly.

The profile at Site 581, which is older than the two preceding sites, shows higher Ti values prior to 5 m.y. ago (Fig. 4). The concentration increases downhole in steps, with an increase of approximately 0.05% at 9 m.y. (225 m) and a similar 0.05% increase at about 14 m.y. (245 m). These increases correspond to the downhole changes in lithology from gray green siliceous clay to light brown pelagic clay to dark brown pelagic clay, respectively (see Site 581 chapter, this volume).

Below 270 m, only chert was recovered from the sedimentary section at Site 581. Ti values for the cherts are three to five times lower than in the overlying sediments (due to dilution by silica), but decrease downhole suggesting a reversal of the lithologic trend observed from 180 to 270 m (Fig. 4). Because the time duration of the

interval represented by the chert section is unknown, we can only infer that the low Ti values at the base of the section are indicative of biogenic dilution of terrigenous debris at the time when the site lay beneath the equatorial zone of high biological productivity.

Other elements with distributions similar to Ti, particularly at Sites 579 and 580, are Al, Mg, K, and Fe (Fig. 2). At Site 581, Fe diverges from Ti in the deeper cherts, reaching up to 50% of the detrital values below 300 m (Fig. 4). One possible explanation for such a divergence would be the deposition of excess hydrothermal Fe beneath the equator (Leinen and Stakes, 1979).

Si, much of which is supplied as biogenic opal, varies almost inversely with the terrigenous elements. Short-term variability is again about 10%, with the more northerly (and more productive) Site 580 showing more variability than Site 579, particularly during the past 1 m.y. (Fig. 2).

At Site 581, the light brown (224–245 m) and gray green (above 224 m) sections and the chert samples (below 276 m) are all silica rich (Fig. 4). In fact, the chert values ( $32.8 \pm 1.3\%$ ) are indistinguishable from those for the light brown pelagic clays ( $31.8 \pm 1.4\%$ ). In contrast, the dark brown pelagic clays (245–276 m) are silica depleted, with a mean value of only 24.2% (and a standard deviation of 2.4%).

Mn and S are both redox-sensitive elements. Mn is reduced from the insoluble +4 to soluble +2 state under mildly reducing (suboxic) conditions (Froelich et al., 1979), whereas S is reduced from +6 to -2 ( $\text{SO}_4^{2-}$  to  $\text{S}^{2-}$ ) only when  $\text{O}_2$ ,  $\text{NO}_3^-$ ,  $\text{Mn}^{4+}$ , and  $\text{Fe}^{3+}$  have been consumed.

At Site 579, virtually all the oxyhydroxide Mn has been reduced and has diffused out of the sediments (Fig. 3). Spikes near the base of the section and near the surface are the only indicators of more oxidized conditions. In contrast, the more rapidly deposited sediments at Site



Table 1. (Continued).

OSU Lab Sample	Core	Section	Depth in Section (m)	Depth in Core (m)	Mn	Fe	Si	Al	K	Ca	Mg	Ti	P	Ba	S
DP10865	8	4	0.57	85.57	0.03	4.88	30.9	8.11	2.51	0.62	2.09	0.374	0.047	0.074	0.260
DP10866	8	5	0.57	87.07	0.01	2.53	33.7	5.66	1.70	0.86	0.85	0.255	0.038	0.075	0.102
DP10867	8	6	0.57	88.57	0.02	3.59	30.7	7.86	2.26	0.79	1.66	0.377	0.047	0.074	0.051
DP10868	8	7	0.37	89.87	0.02	3.51	32.6	6.92	2.06	0.53	1.39	0.327	0.043	0.077	0.037
DP10869	9	1	1.23	91.23	0.04	3.19	32.5	7.21	2.21	0.63	1.27	0.304	0.041	0.077	0.022
DP10870	9	2	0.91	92.41	0.04	3.34	32.3	6.52	1.89	0.65	1.16	0.288	0.039	0.076	0.019
DP10871	9	3	0.91	93.91	0.01	3.25	32.5	6.86	2.22	0.55	1.16	0.275	0.041	0.087	0.031
DP10872	9	4	1.19	95.69	0.05	3.73	33.5	7.02	2.07	0.99	1.16	0.309	0.043	0.075	0.047
DP10873	9	5	0.91	96.91	0.02	3.83	32.9	6.74	2.07	0.65	1.26	0.308	0.042	0.073	0.014
DP10874	10	1	0.55	100.05	0.07	3.73	32.9	6.57	2.04	0.49	1.34	0.292	0.040	0.085	0.026
DP10875	10	2	0.55	101.55	0.04	3.07	30.4	5.78	1.55	0.61	1.03	0.253	0.037	0.067	0.013
DP10876	10	3	0.55	103.05	0.05	3.32	32.7	6.43	1.97	0.67	1.21	0.287	0.040	0.079	0.023
DP10877	10	4	0.55	104.55	0.04	4.21	32.6	7.15	2.07	0.59	1.41	0.324	0.039	0.091	0.033
DP10878	10	5	0.55	106.05	0.03	3.65	32.0	6.36	1.99	0.64	1.23	0.291	0.037	0.071	0.051
DP10879	11	1	0.99	109.99	0.08	3.86	32.2	7.68	2.16	0.46	1.53	0.324	0.042	0.072	0.023
DP10880	11	2	0.99	111.49	0.05	3.67	33.1	6.85	1.94	0.47	1.35	0.299	0.039	0.085	0.027
DP10881	11	3	0.99	112.99	0.08	3.11	33.8	5.76	1.76	0.29	1.16	0.256	0.036	0.065	0.035
DP10882	11	4	0.99	114.49	0.05	3.20	33.7	6.68	2.04	0.43	1.29	0.279	0.039	0.065	0.064
DP10883	11	5	0.71	115.71	0.12	2.87	35.6	5.26	1.61	0.31	1.05	0.239	0.037	0.072	0.020
DP10884	12	1	0.87	119.37	0.06	2.75	33.3	5.42	1.95	0.28	0.94	0.221	0.035	0.064	0.012
DP10885	12	2	0.87	120.87	0.03	3.52	34.3	6.50	2.11	0.22	1.33	0.294	0.039	0.090	0.019
DP10886	12	3	0.87	122.37	0.02	3.26	33.0	6.05	1.89	0.30	1.25	0.279	0.036	0.093	0.059
DP10887	12	4	0.87	123.87	0.02	3.71	33.1	6.64	1.94	0.45	1.29	0.295	0.038	0.070	0.013
DP10888	12	5	0.85	125.35	0.01	3.27	32.2	6.41	1.88	0.48	1.28	0.294	0.036	0.086	0.039
DP10889	12	6	0.07	126.07	0.04	4.09	31.5	6.32	1.83	0.95	1.30	0.306	0.041	0.065	0.051
DP10890	13	1	0.42	128.42	0.02	2.29	32.4	5.66	2.23	0.29	0.88	0.192	0.034	0.067	0.120
DP10891	13	2	0.42	129.92	0.07	3.35	33.4	5.65	1.74	0.27	1.15	0.254	0.035	0.095	0.012
DP10892	13	3	0.42	131.42	0.07	3.49	32.7	6.33	1.87	0.29	1.29	0.274	0.036	0.070	0.087
DP10893	13	4	0.42	132.92	0.02	3.24	33.4	6.15	1.88	0.31	1.20	0.280	0.036	0.069	0.055
DP10894	13	5	0.42	134.42	0.03	3.46	33.2	6.30	1.82	0.38	1.24	0.287	0.035	0.063	0.060
DP10895	14	1	0.81	138.31	0.01	2.63	31.9	5.30	1.83	0.25	0.90	0.238	0.033	0.071	0.051
DP10896	14	2	0.81	139.81	0.05	3.02	33.6	5.89	1.80	0.40	1.08	0.263	0.035	0.072	0.189
DP10897	14	3	0.81	141.31	0.02	3.01	33.8	5.95	1.84	0.28	1.12	0.265	0.035	0.075	0.192
DP10898	14	4	0.81	142.81	0.01	2.13	28.5	4.14	1.45	0.25	0.70	0.162	0.026	0.053	0.190
DP10899	14	5	0.81	144.31	0.23	3.21	36.3	7.07	2.09	0.36	1.30	0.315	0.041	0.082	0.030
DP10900	15	1	0.89	147.89	0.01	4.08	34.7	8.42	2.48	0.31	1.60	0.350	0.044	0.097	0.020
DP10901	15	2	0.21	148.71	0.03	3.60	32.2	7.55	2.26	0.41	1.36	0.304	0.038	0.080	0.022

Note: Samples DP10808-10819 are from Hole 579, subsequent samples are from Hole 579A.

580 contain higher and more variable amounts of Mn (Fig. 3). Given the gray green color of the Site 580 sediments, which implies  $\text{Fe}^{3+}$  reduction (Lyle, 1983), we are more inclined to assign the higher Mn values to the presence of  $\text{MnCO}_3$  than to oxyhydroxides. We have not been able to identify  $\text{MnCO}_3$  in X-ray diffractograms, because of its low concentration, but Coleman et al.'s (1982) description of  $\text{MnCO}_3$  in similar reduced sediments collected on Leg 68 (Pedersen and Price, 1982) and the availability of  $\text{CO}_3^{2-}$  at Site 580 (inferred from the Ca concentrations) add credibility to this hypothesis.

At Site 581, the Mn profile can be divided into three segments (Fig. 4). Above 224 m, in the gray green sediments, Mn values (with one exception) are very low, comparable to those at Sites 579 and 580. In this interval, oxyhydroxide Mn has been reduced and lost from the sediments. The residual detrital Mn is somewhat diluted

by biogenic opal. From 224 to 245 m, in the light brown siliceous clay, some reduction may have taken place, but there is less opal dilution. From 245 to 276 m, authigenic Mn-oxyhydroxides form a much larger fraction of the dark brown pelagic clay, which accumulated more slowly and is strongly oxidizing. The Mn contents of the Site 581 cherts (276–343 m) are variable, but generally fairly high (comparable to the light brown siliceous clays), suggesting that the silicified clays were more like the sediments below 224 m than the shallower deposits at Site 581.

The elements Ba, P, and Ca, which, like Si, are associated with biogenic deep-sea deposition, have distributions intermediate between those of Ti-Al and Si. At Sites 579 and 580, P resembles Ti, whereas Ba resembles Si (although values at Site 580 are distinctly higher and more variable than those at Site 579; Fig. 3). Ca has its own distribution, with high variability at both sites, and



Table 2. (Continued).

OSU Lab Sample	Core	Section	Depth in Section (m)	Depth in Core (m)	Mn	Fe	Si	Al	K	Ca	Mg	Ti	P	Ba	S
DP10954	11	4	0.44	93.74	0.07	3.60	32.4	6.66	2.13	0.61	1.58	0.322	0.043	0.088	0.351
DP10955	11	5	0.44	95.24	0.22	3.19	34.8	6.15	1.89	0.54	1.43	0.290	0.041	0.131	0.124
DP10956	12	1	1.11	99.41	0.07	2.56	33.9	5.01	1.71	0.43	1.03	0.227	0.036	0.087	0.231
DP10957	12	2	1.11	100.91	0.13	2.82	33.5	4.34	1.43	1.49	1.14	0.219	0.035	0.093	0.486
DP10958	12	3	0.81	102.11	0.09	2.58	34.2	5.23	2.01	0.49	1.10	0.226	0.037	0.111	0.144
DP10959	12	4	1.11	103.91	0.03	2.83	33.8	5.29	1.64	0.37	1.12	0.242	0.038	0.127	0.132
DP10960	12	5	0.96	105.26	0.14	4.05	32.3	7.43	2.29	0.67	1.85	0.352	0.045	0.071	0.525
DP10961	12	6	1.11	106.91	0.14	3.19	33.8	6.12	1.92	0.78	1.32	0.279	0.042	0.108	0.145
DP10962	13	1	1.11	108.91	0.06	3.42	33.6	4.78	1.56	0.33	1.14	0.224	0.035	0.116	0.516
DP10963	13	2	1.11	110.41	0.09	2.89	36.4	4.25	1.43	0.26	1.04	0.202	0.038	0.119	0.103
DP10964	13	3	1.11	111.91	0.08	2.72	35.3	4.37	1.46	0.28	1.07	0.214	0.038	0.121	0.089
DP10965	13	4	1.11	113.41	0.09	3.38	34.0	5.66	1.49	1.22	1.13	0.256	0.042	0.062	0.315
DP10966	13	5	1.11	114.91	0.12	3.02	34.0	5.42	1.71	0.45	1.27	0.238	0.038	0.126	0.255
DP10967	13	6	1.11	116.41	0.12	3.44	31.6	6.02	1.89	1.39	1.44	0.280	0.040	0.082	0.532
DP10968	14	1	1.16	118.46	0.14	3.83	33.7	5.32	1.64	0.64	1.39	0.252	0.038	0.120	1.450
DP10969	14	2	1.16	119.96	0.11	2.38	33.6	4.84	1.65	0.90	0.86	0.204	0.035	0.085	0.117
DP10970	14	3	1.16	121.46	0.05	3.65	32.9	6.31	1.96	0.46	1.49	0.280	0.040	0.130	0.202
DP10971	14	4	1.16	122.96	0.15	3.21	35.2	4.87	1.55	0.29	1.24	0.233	0.036	0.130	0.231
DP10972	14	5	1.16	124.46	0.09	3.12	34.0	5.73	1.80	0.42	1.29	0.278	0.039	0.103	0.243
DP10973	14	6	1.16	125.96	0.12	3.10	33.4	5.66	1.85	0.32	1.43	0.267	0.037	0.116	0.099
DP10974	15	1	0.58	127.38	0.10	3.53	32.3	6.65	2.12	0.41	1.57	0.302	0.039	0.103	0.151
DP10975	15	2	0.58	128.88	0.05	2.54	33.7	5.16	1.71	0.53	0.91	0.212	0.035	0.105	0.002
DP10976	15	3	0.58	130.38	0.08	2.70	33.7	5.13	1.60	0.40	1.07	0.225	0.034	0.089	0.044
DP10977	15	4	0.58	131.88	0.10	3.09	33.9	5.49	1.74	0.33	1.19	0.255	0.037	0.114	0.196
DP10978	15	5	0.58	133.38	0.08	2.82	33.4	5.61	1.77	0.60	1.05	0.253	0.037	0.083	0.012
DP10979	15	6	0.58	134.88	0.10	2.59	32.7	5.57	2.10	0.71	0.95	0.185	0.033	0.075	0.019
DP10980	16	1	0.81	137.11	0.14	3.70	33.5	5.76	1.75	0.24	1.42	0.251	0.036	0.112	0.005
DP10981	16	2	0.81	138.61	0.13	3.20	41.2	5.43	1.84	0.35	1.32	0.277	0.045	0.113	0.150
DP10982	16	3	0.81	140.11	0.12	2.53	35.4	4.72	1.53	0.30	1.11	0.221	0.034	0.103	0.033
DP10983	16	4	0.81	141.61	0.05	2.94	34.7	5.48	1.69	0.33	1.18	0.239	0.037	0.092	0.012
DP10984	16	5	0.81	143.11	0.05	2.45	35.3	3.06	1.06	0.08	0.72	0.152	0.030	0.092	0.212
DP10985	16	6	0.81	144.61	0.05	2.27	34.8	4.18	1.44	0.21	0.90	0.203	0.031	0.080	0.032
DP10986	17	1	0.78	146.58	0.06	2.31	34.5	4.37	1.59	0.39	0.77	0.190	0.035	0.111	0.000
DP10987	17	2	0.78	148.08	0.05	2.88	33.8	4.85	1.53	0.27	1.11	0.229	0.031	0.123	0.079
DP10988	17	3	0.78	149.58	0.03	2.59	34.5	4.93	1.67	0.27	1.03	0.220	0.033	0.129	0.038
DP10989	17	4	0.78	151.08	0.04	2.79	33.3	6.01	2.11	0.48	1.14	0.236	0.034	0.096	0.065
DP10990	17	5	0.78	152.58	0.11	2.96	33.3	5.76	1.73	0.53	1.22	0.262	0.035	0.096	0.103

a well-defined decrease in concentration below about 3.2 m.y. (110 m) at Site 579 and about 2.3 m.y. (100 m) at Site 580.

At Site 581, Ba, P, and Ca all resemble Ti rather than Si in the clay section. In the basal dark brown pelagic clay (245–276 m) and in the upper and lower cherts (below 276 m), however, P has clear peaks that are matched by Ca peaks, suggesting abundant fish debris. Ba also peaks in the lower cherts, but not the upper ones. Ba peaks in the oxidized (light and dark brown) pelagic clays, as it does elsewhere in the Pacific (Dymond, 1981; Leinen, 1979).

Because elements like silicon are derived from more than one source (detrital aluminosilicates and biogenic opal, for example), we have carried out a Q-mode factor analysis of the data. In its conventional form (Klovan and Imbrie, 1971), such a factor analysis expresses each sample in terms of a number of orthogonal functions

that share the variance of the data set as equally as possible. This procedure simplifies the interpretation of large data sets, but the factors may be difficult to interpret physically because they can contain negative contributions of some elements.

Figure 5 shows the downhole variation in three factors derived from the data sets for both Sites 579 and 580. Overall, it is clear that the sediments at Site 579 are markedly less variable than those at Site 580. The variability is due primarily to Mn (Factor 2), which is relatively uniform at Site 579 (particularly above 80 m), but fluctuates markedly at Site 580 (Fig. 3). In contrast, the biogenically dominated Factor 3 (loaded in Si and Ba; Fig. 5) is of comparable importance at the two sites. In fact, this factor is slightly more variable at Site 579.

The factors are easier to interpret if the Q-mode axes are rotated toward the mean of the data set until they enter the positive quadrant (i.e., until their projections



Table 3. (Continued).

OSU Lab Sample	Core Section	Depth in Section (m)	Depth in Core (m)	Mn	Fe	Si	Al	K	Ca	Mg	Ti	P	Ba	S	
DP11053	8	5	1.01	245.51	0.61	4.86	23.8	7.19	2.06	0.30	1.71	0.342	0.043	0.174	0.036
DP11054	9	1	0.25	248.25	0.60	4.97	25.5	7.81	2.21	0.32	1.93	0.357	0.051	0.198	0.045
DP11055	9	1	0.73	248.73	0.90	4.66	24.9	7.62	2.02	0.27	1.90	0.327	0.043	0.162	0.033
DP11056	9	1	1.29	249.29	0.75	4.73	23.8	7.37	2.07	0.29	1.81	0.332	0.051	0.121	0.016
DP11057	9	2	0.25	249.75	0.87	4.97	23.8	7.29	2.09	0.33	1.79	0.343	0.047	0.149	0.030
DP11058	9	2	0.73	250.23	0.93	4.84	27.6	8.51	2.24	0.31	2.14	0.352	0.055	0.194	0.042
DP11059	9	2	1.29	250.79	0.77	4.86	24.9	7.55	2.22	0.30	1.92	0.346	0.044	0.218	0.042
DP11060	9	3	0.25	251.25	0.99	4.83	24.2	7.52	2.17	0.33	1.85	0.330	0.065	0.232	0.041
DP11061	9	3	0.73	251.73	1.06	4.77	23.2	7.24	2.11	0.27	1.80	0.320	0.057	0.212	0.017
DP11062	9	4	0.25	252.75	1.30	4.97	25.9	8.09	2.33	0.43	1.85	0.339	0.077	0.171	0.026
DP11063	9	4	0.73	253.23	1.13	4.75	24.6	7.77	2.15	0.35	1.80	0.332	0.063	0.156	0.026
DP11064	10	1	0.11	257.61	1.35	5.03	23.6	8.18	2.27	0.30	1.81	0.349	0.061	0.113	0.006
DP11065	10	1	0.81	258.31	1.56	4.85	23.4	8.06	2.18	0.41	1.81	0.353	0.082	0.130	0.016
DP11066	10	1	1.41	258.91	1.73	4.99	19.7	6.94	1.96	0.31	1.46	0.343	0.058	0.102	0.007
DP11067	10	2	0.11	259.11	1.66	4.29	22.2	7.93	2.01	0.40	1.48	0.292	0.078	0.120	0.014
DP11068	10	2	0.81	259.81	2.61	4.73	22.3	8.10	2.43	0.57	1.55	0.317	0.174	0.112	0.023
DP11069	10	2	1.41	260.41	2.35	4.77	21.4	7.81	2.25	0.38	1.67	0.343	0.107	0.103	0.000
DP11070	10	3	0.11	260.61	2.91	5.20	21.7	8.21	2.41	0.58	1.71	0.355	0.181	0.085	0.021
DP11071	10	3	0.81	261.31	2.05	4.67	21.9	7.92	2.58	0.59	1.90	0.341	0.178	0.041	0.021
DP11072	10	3	1.31	261.81	1.62	5.47	20.1	7.08	2.07	0.76	1.72	0.493	0.229	0.044	0.025
DP11073	10	4	0.11	262.11	1.39	4.96	22.8	7.66	2.08	0.29	1.76	0.340	0.059	0.128	0.023
DP11074	10	4	0.61	262.61	1.82	5.18	28.1	9.28	2.34	0.33	2.29	0.380	0.070	0.189	0.025
DP11075	10	5	0.11	263.61	1.25	5.02	26.1	8.74	2.38	0.32	2.06	0.371	0.062	0.130	0.026
DP11076	10	5	0.61	264.11	0.99	4.83	23.8	7.96	2.25	0.29	1.84	0.353	0.056	0.110	0.022
DP11077	10	6	0.11	265.11	1.29	4.94	27.2	8.78	2.32	0.32	2.07	0.358	0.069	0.162	0.032
DP11078	11	1	0.17	267.17	1.85	5.07	24.1	8.60	2.79	0.55	2.12	0.392	0.186	0.044	0.026
DP11079	12	1	0.21	276.71	0.11	1.16	33.9	1.08	0.47	0.68	0.42	0.085	0.248	0.003	0.023
DP11080	12	1	0.37	276.87	0.00	1.40	33.3	1.15	0.56	0.49	0.45	0.091	0.186	0.000	0.016
DP11081	13	1	0.04	286.04	0.00	0.32	31.3	0.21	0.17	0.23	0.04	0.091	0.117	0.000	0.016
DP11082	14	1	0.22	295.72	0.34	1.71	33.5	0.77	0.42	0.28	0.33	0.059	0.117	0.029	0.008
DP11083	15	1	0.34	305.34	0.51	2.35	33.5	0.19	0.17	0.25	0.07	0.040	0.086	0.035	0.006
DP11084	15	1	0.95	305.95	0.37	2.11	31.3	0.27	0.22	0.21	0.07	0.031	0.080	0.024	0.005
DP11085	16	1	0.23	314.72	0.68	2.58	34.2	0.61	0.42	0.53	0.30	0.051	0.182	0.119	0.022
DP11086	17	1	0.12	324.12	0.15	1.67	33.3	0.19	0.24	0.19	0.09	0.026	0.089	0.095	0.041
DP11087	17	1	0.30	324.30	0.00	1.76	34.0	0.22	0.25	0.10	0.11	0.026	0.051	0.000	0.000
DP11088	17	1	1.10	325.10	0.31	2.24	32.6	0.14	0.11	0.04	0.03	0.037	0.031	0.000	0.000
DP11089	18	1	0.19	333.69	0.44	1.93	29.9	0.13	0.10	0.05	0.02	0.020	0.033	0.000	0.000

on all elemental abundance axes are positive). These rotated axes can then be converted to actual elemental compositions and can be treated as physical end members of the population. This technique was developed by Leinen and Pisias (1984). We have used their algorithm to analyze the Leg 86 data.

Table 4 shows the compositions of the reference (rotated) axes for the combined Site 579 and 580 data sets. Figure 6 shows how these factors load on to the down-hole samples.

Factor 1 is primarily terrigenous detritus with some biogenic opal. The Site 580 samples are slightly depleted in this factor and are markedly more variable than the Site 579 samples (Fig. 6). In contrast, Factor 3, which is dominated by biogenic opal and Mn, is much more abundant in the Site 580 samples from the more productive

northern site. Factor 2 is a mixture of authigenic iron sulfide and terrigenous detritus. Its greater abundance at Site 580 is consistent with a greater influx of organic carbon, which has served as the energy source for sulfate-reducing bacteria at this site.

If sulfur is excluded from the factor analysis, three simpler end members emerge (Table 5, Fig. 7). Factor 1 is again dominated by terrigenous debris, in this case with a smaller addition of biogenic opal. The downhole patterns at Sites 579 and 580 are very similar, with the abundance of factor 1 roughly doubling from the oldest (Pliocene) to youngest (Quaternary) samples. The opal-rich Factor 3 shows almost the inverse pattern, with a marked decrease from older to younger samples. At Site 580, the transition is continuous, with a lot of variability throughout the section. In contrast, the abundance of

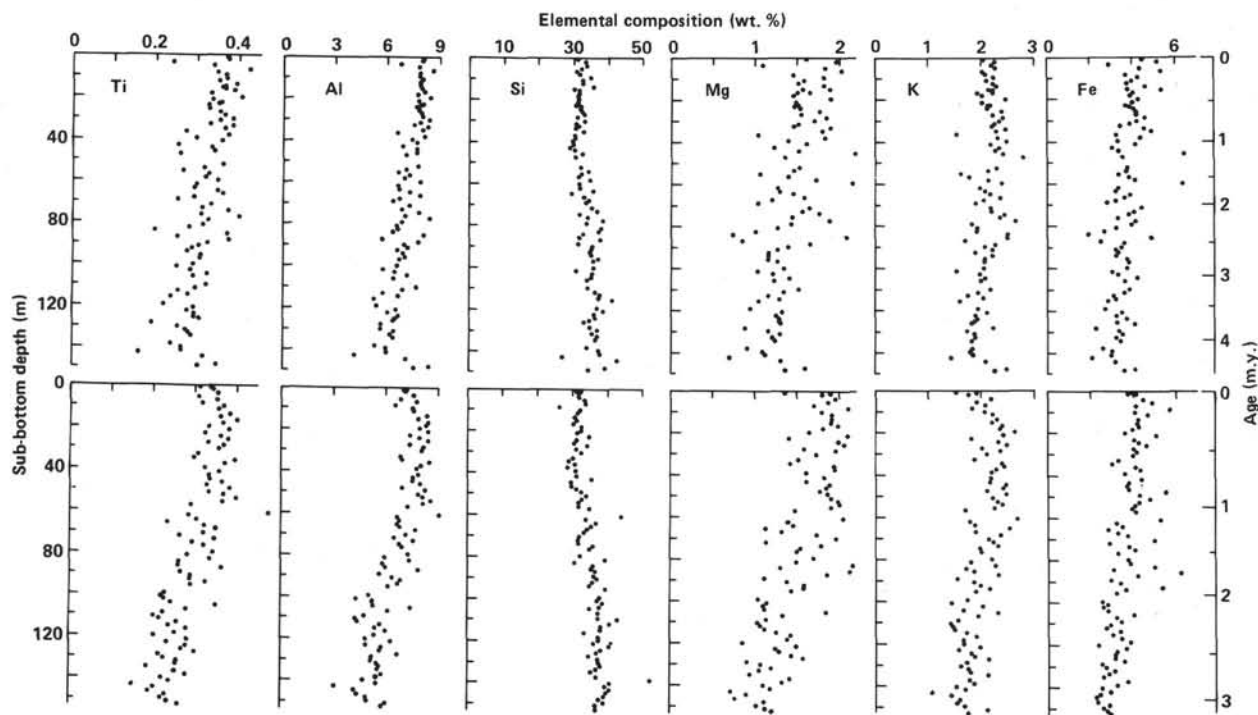


Figure 2. Downhole profiles of elemental abundances in samples from Sites 579 (upper) and 580 (lower). Analyses by X-ray fluorescence, salt corrected. The data are given in Tables 1 and 2.

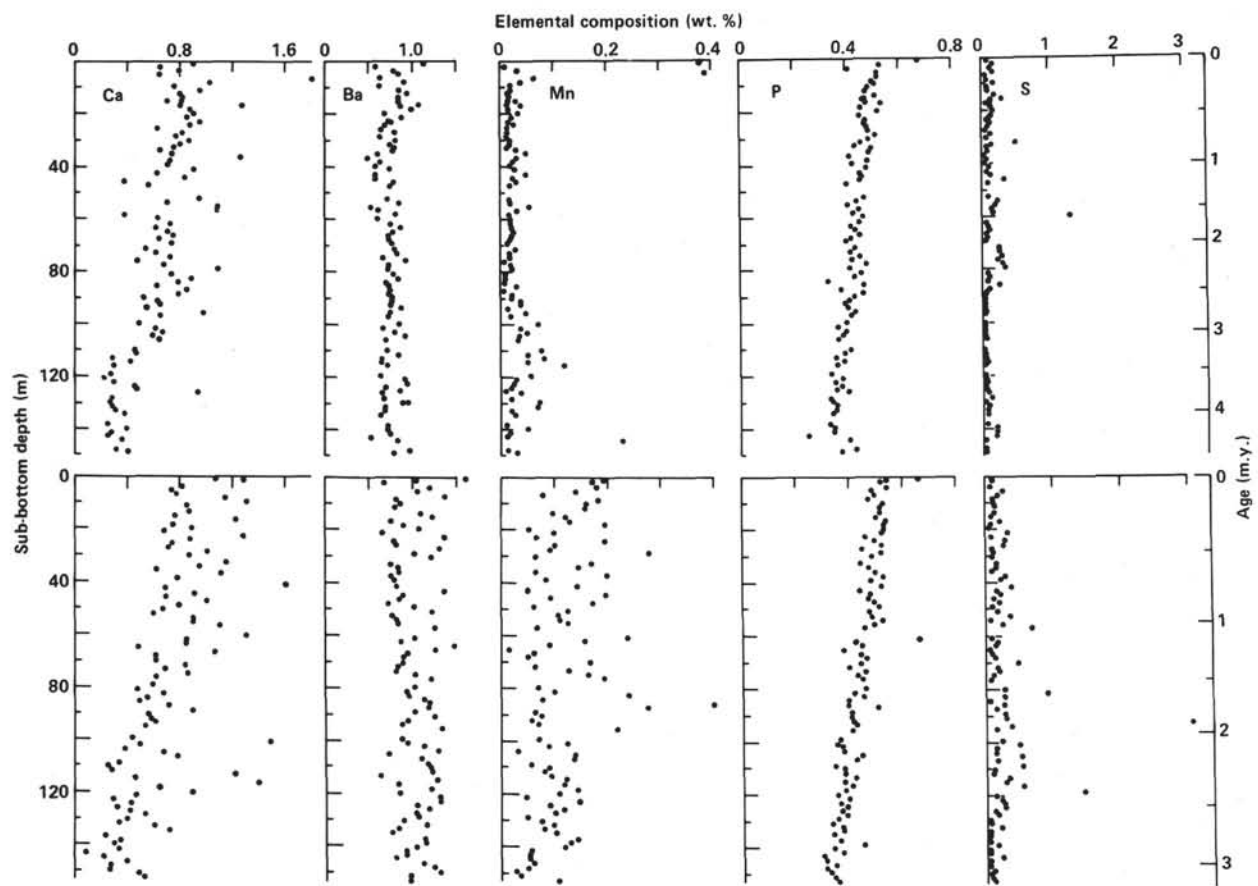


Figure 3. Downhole profiles of minor element abundances in samples from Sites 579 (upper) and 580 (lower). Analyses by X-ray fluorescence, salt corrected. The data are given in Tables 1 and 2.

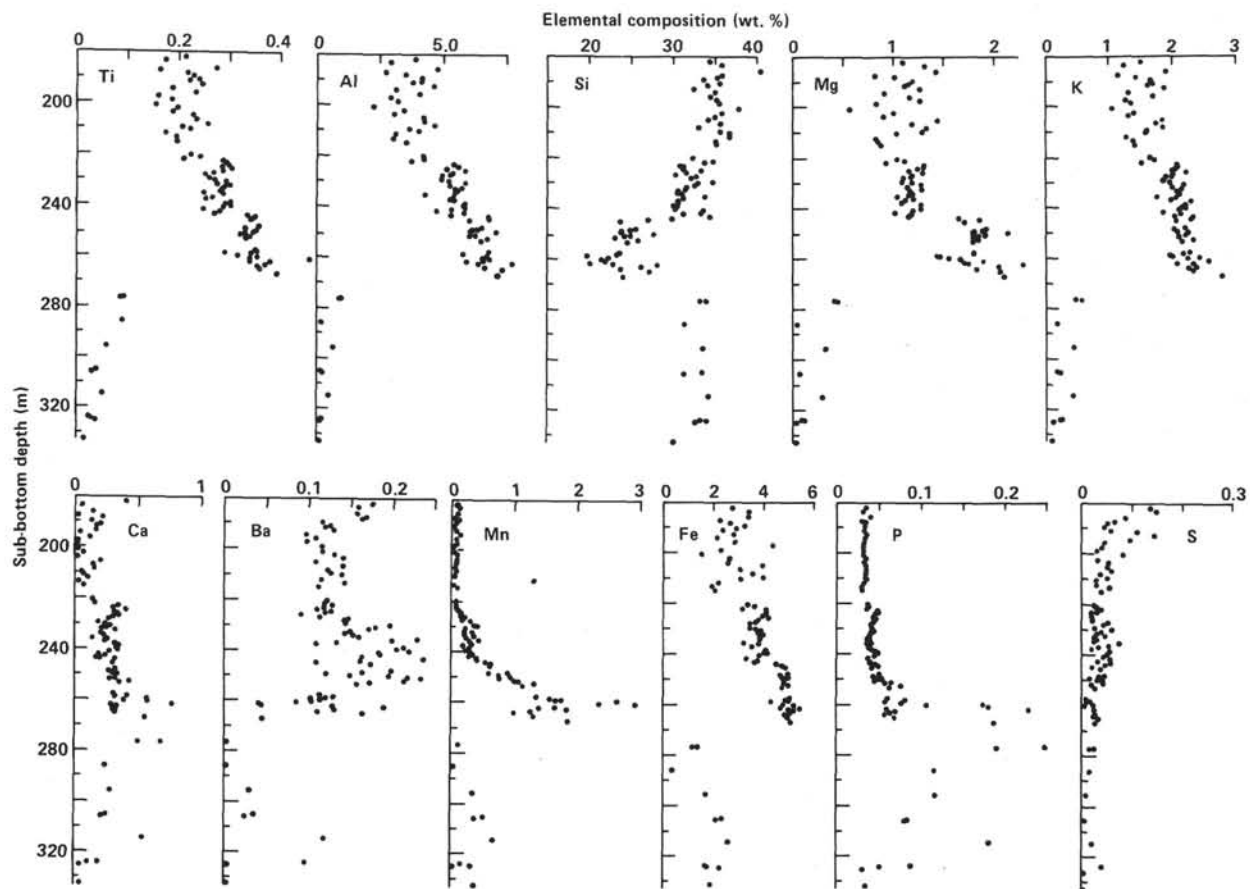


Figure 4. Downhole profiles of elemental abundances in samples from Site 581. Analyses by X-ray fluorescence, salt corrected. The data are given in Table 3.

Factor 3 at Site 579 decreases abruptly near 110 m, corresponding to an age of about 3.2 m.y. Factor 2, which consists of terrigenous detritus enriched in authigenic (?) iron and manganese, is more abundant at Site 580 than at Site 579, but shows little variation downhole.

The results of factor analysis of the Site 581 samples are shown in Figure 8. The Q-mode analysis (Table 6) distinguishes detrital, Mn-rich, and biogenic factors (Factors 1, 2, and 3, respectively). The detrital factor decreases continuously in importance from the basal clays to the cherts below 276 m. The other two factors show sharp discontinuities at this boundary.

The rotated factors (Table 7), in contrast, vary much more smoothly across the clay/chert boundary. The detrital-rich Factor 1 decreases to very low values in the chert, with only three elevated values near 325 m. Factor 3, dominated by opal and minor fish debris, is uniformly high in the chert, decreases to a minimum in the dark brown clays (245–276 m), and increases slightly in the less oxidized clays. Factors 2, which is dominated by an authigenic ferromanganese component with subordinate fish debris and detritus, is concentrated in the dark brown clays (245–276 m). Lower but still significant levels are evident in the light brown clays (224–245 m) and chert (below 276 m). Only the reduced (gray green) clays above 224 m are depleted in this factor.

## DISCUSSION AND CONCLUSIONS

The elemental composition of sediments at Sites 579, 580, and 581 is dominated by contributions from terrigenous detritus and opal-rich biogenic debris. Redox-driven diagenetic reactions (mobilization and redistribution of manganese and precipitation of iron sulfide) and the deposition of authigenic ferromanganese oxyhydroxides in mid-Tertiary dark brown clays at Site 581 modify the abundances of some elements.

From a geochemical perspective, Sites 579 and 580 are almost indistinguishable. A slight enrichment of the biogenically associated elements Si, Ca, Ba, and P at Site 580, which lies beneath more biologically productive waters than Site 579, is the major difference. At both sites, the ratio of detrital to biogenic debris increases uphole from the late Pliocene to the late Quaternary portions of the profiles. It seems unlikely that this trend resulted from a decrease in biogenic input, given the northward drift of the sites and more vigorous oceanic circulation during the Quaternary in this region. Rather, the trend probably reflects the accelerated eolian deposition of continental debris from loess deposits in Asia that accompanied the development of Northern Hemisphere glaciation and that has been recognized elsewhere in the North Pacific (Heath, 1969; Leinen and Heath, 1981).

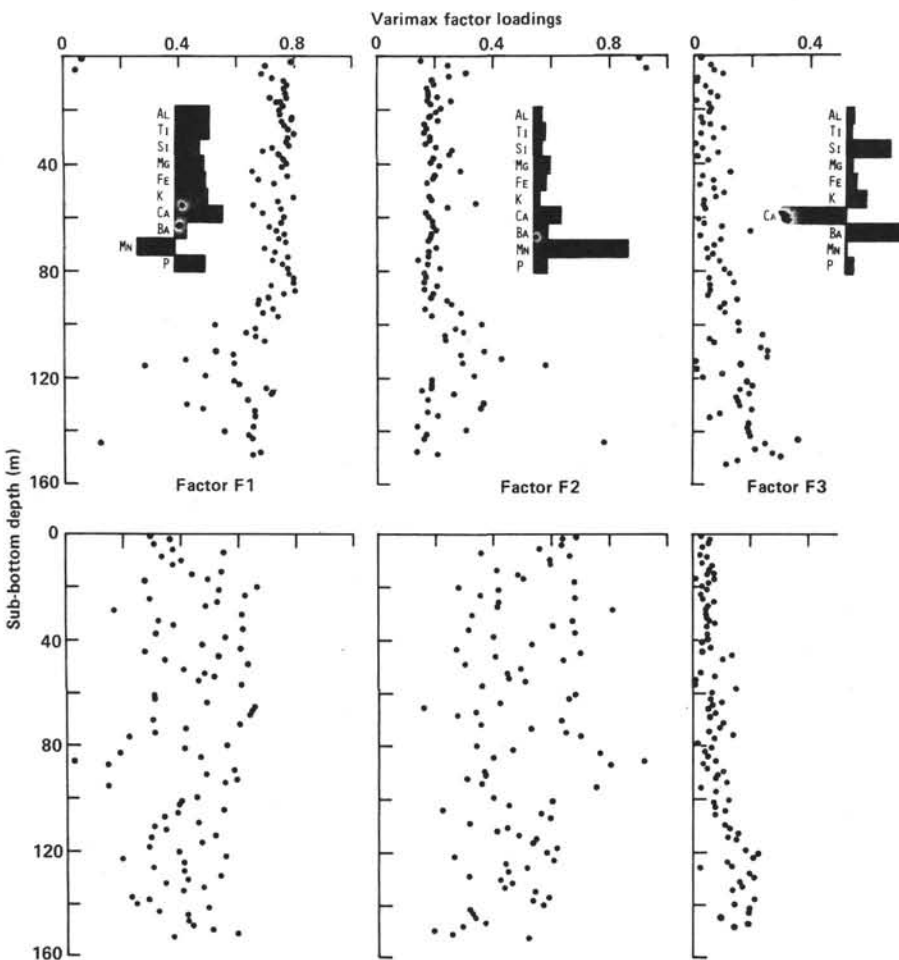


Figure 5. Downhole profiles of loadings of Q-mode varimax factors on samples from Sites 579 (upper) and 580 (lower). Histograms show contributions of elements to each factor.

Table 4. Composition (wt. %) of the rotated Q-mode factors for Sites 579 and 580 plotted in Figure 6.

Element	Factor 1	Factor 2	Factor 3
Ti	0.31	0.35	0.25
Al	7.09	6.53	5.18
Si	32.4	25.3	34.3
Mg	1.35	2.65	1.62
K	2.14	1.83	1.53
Fe	3.51	6.36	3.48
Ca	0.65	1.39	0.62
Ba	0.08	0.07	0.14
Mn	0.00	0.005	0.48
P	0.04	0.05	0.04
S	0.03	3.08	0.00

A feature deserving of additional study is the enhanced deposition of Mn at Site 580 relative to Site 579. We suspect that the excess Mn is preserved as a carbonate, but the depositional conditions responsible for such preservation have not been identified.

The record at Site 581 captures the basal part of the sequence cored at Sites 579 and 580 (reduced, opal-bearing detrital clays), as well as oxidized detrital-rich clays and highly oxidized pelagic clays rich in authigenic fer-

romanganese oxyhydroxides. This section overlies porcellaneous chert.

The oxidized clays are reminiscent of "red clay" sequences elsewhere in the North Pacific (see Site 576 and 578 chapters, this volume; Leinen, 1979). Both P and Ba are enriched in the darkest brown clays, reflecting the concentration of the most refractory biogenic debris (phosphatic fish fragments and barite) in the least rapidly accumulating sediments.

The porcellaneous cherts at Site 581 contain some surprises. They contain about the same concentration of silica as the oxidized detrital clays and markedly less than the biosiliceous clays at Site 580. The relatively high Mn contents and red to yellow colors also point to fairly slow deposition in a well-oxygenated environment. The high P contents of the cherts, particularly the youngest ones, also is suggestive of slow deposition (i.e., greater relative abundance of phosphatic fish debris). The possibility that precipitation of the chert layers concentrates fish debris (perhaps by physically displacing the finer clay particles) cannot be excluded, however.

Overall, the chemical data are consistent with the paleoceanographic interpretations derived from lithologic and paleontologic descriptions of the sections at Sites

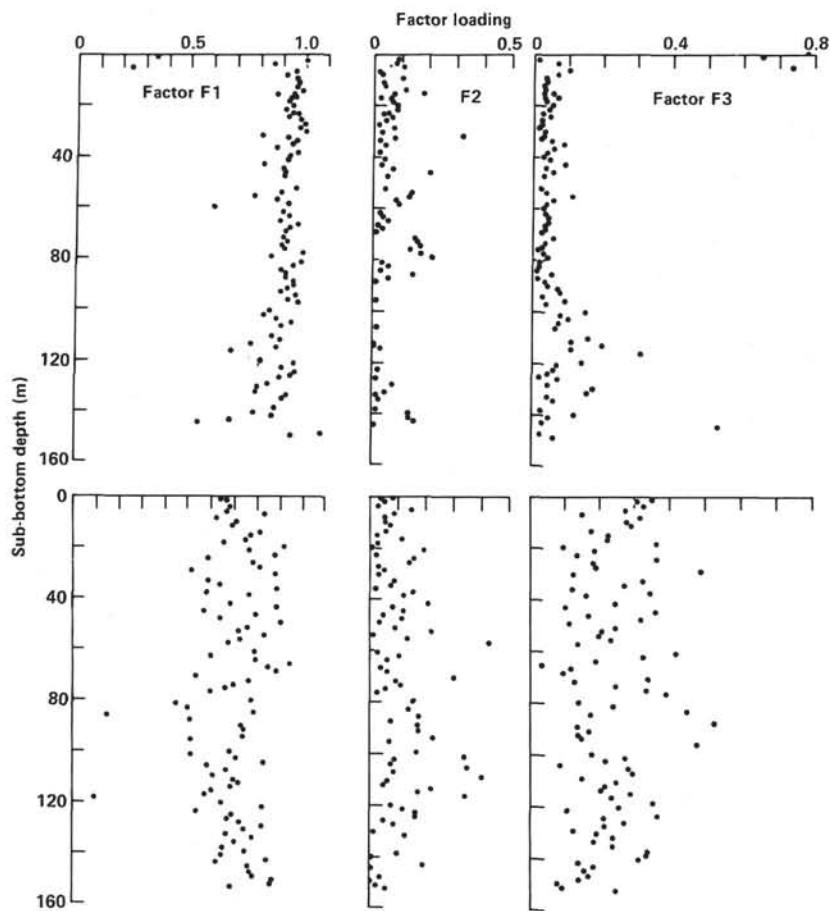


Figure 6. Downhole profiles of loadings of rotated varimax factors (see text for explanation) on samples from Sites 579 (upper) and 580 (lower). Compositions of rotated factors are listed in Table 4. All elements, including sulfur, are included.

Table 5. Composition (wt. %) of the rotated Q-mode factors (S omitted) for Sites 579 and 580 plotted in Figure 7.

Element	Factor 1	Factor 2	Factor 3
Ti	0.34	0.35	0.23
Al	7.75	6.57	5.16
Si	30.7	28.2	36.0
Mg	1.52	2.63	1.10
K	2.22	1.38	1.81
Fe	3.91	5.15	2.90
Ca	0.94	2.10	0.00
Ba	0.07	0.14	0.11
Mn	0.00	0.90	0.06
P	0.05	0.06	0.03

579, 580, and 581. The sets of closely spaced analyses presented here yield a measure of both the general trends and variability of deposition at the three sites. This data set should also be useful for future studies of the comparative geochemistry of North Pacific pelagic clays.

#### ACKNOWLEDGMENTS

We are grateful to the members of the scientific party of Leg 86 for discussions concerning the deposition of western North Pacific pelagic sediments. We also acknowledge the assistance of Ivan Pavlov and

Greg Campi in preparing and analyzing samples, and helping to plot the results. This manuscript was improved by the reviews of Miriam Kastner and Mitchell Lyle.

#### REFERENCES

- Chase, T. E., 1975. Topography of the oceans. Univ. Calif. San Diego, Scripps Inst. Oceanogr., *Inst. Mar. Resources Tech. Rept.*, Ser. TR57.
- Coleman, M., Fleet, A., and Donson, P., 1982. Preliminary studies of manganese-rich carbonate nodules from Leg 68, Site 503, eastern equatorial Pacific. In Prell, W. L., Gardner, J. V., et al., *Init. Repts. DSDP*, 68: Washington (U.S. Govt. Printing Office), 481-489.
- Criss, J. W., Birks, L. S., and Gilfrich, J. V., 1978. A versatile x-ray analysis program combining fundamental parameters and empirical coefficients. *Anal. Chem.*, 50:33.
- Dymond, J., 1981. The geochemistry of Nazca Plate surface sediments: an evaluation of hydrothermal, biogenic, detrital and hydrogenous sources. *Mem. Geol. Soc. Am.*, 154:133-173.
- Froelich, P., Klinkhammer, G., Bender, M., Luedtke, N., Heath, R., Cullen, D., Dauphin, P., Hammond, D., Hartman, B., and Maynard, V., 1979. Early oxidation of organic matter in pelagic sediments of the eastern equatorial Atlantic: suboxic diagenesis. *Geochim. Cosmochim. Acta*, 43:1075-1090.
- Heath, G. R., 1969. Mineralogy of Cenozoic deep-sea sediments from the equatorial Pacific Ocean. *Geol. Soc. Am. Bull.*, 80:1997-2018.
- Klovan, J. E., and Imbrie, J., 1971. An algorithm and FORTRAN IV program for large scale Q-mode factor analysis. *J. Int. Assoc. Math. Geol.*, 3:61-77.
- Leinen, M., 1979. Paleochemical signatures in Cenozoic Pacific sediments [Ph.D. dissert.]. University of Rhode Island, Narragansett.

- Leinen, M., and Heath, G. R., 1981. Sedimentary indicators of atmospheric activity in the northern hemisphere during the Cenozoic. *Palaeogeogr., Palaeoclimatol., Palaeoecol.*, 36:1-21.
- Leinen, M., and Pisias, N. G., 1984. An objective technique for determining end-member compositions and for partitioning sediments according to their sources. *Geochim. Cosmochim. Acta*, 48:47-63.
- Leinen, M., and Stakes, D., 1979. Metal accumulation rates in the central equatorial Pacific during Cenozoic time. *Geol. Soc. Am. Bull.*, 90:357-375.
- Lyle, M. W., 1983. The brown-green color transition in marine sediments: a marker of the Fe(III)-Fe(II) redox boundary. *Limnol. Oceanogr.*, 28:1026-1033.
- Pederson, T. F., and Price, N. B., 1982. The geochemistry of manganese carbonate in Panama Basin sediments. *Geochim. Cosmochim. Acta*, 46:59-68.

Date of Initial Receipt: 1 May 1984

Date of Acceptance: 25 September 1984

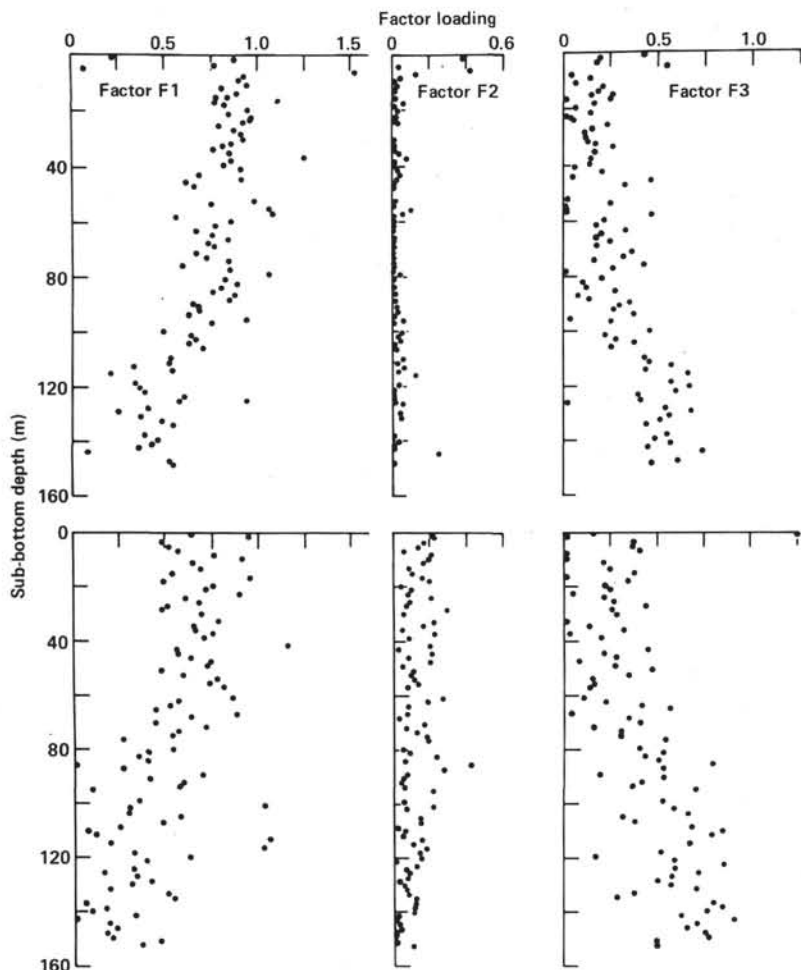


Figure 7. As Figure 6, but for factors that do not include sulfur (see Table 5 for factor compositions).

Table 6. Elemental contributions (factor scores) to Q-mode varimax factors for Site 581 analyses (Fig. 8).

Element	Factor 1	Factor 2	Factor 3
Ti	1.04	0.54	-0.20
Al	1.05	0.68	-0.45
Si	1.27	-0.01	1.37
Mg	1.02	0.66	-0.36
K	1.17	0.43	-0.27
Ca	0.16	0.70	1.19
Ba	1.49	0.10	-0.33
Mn	-0.87	2.72	0.02
Fe	0.88	0.51	0.23
P	-0.11	0.26	2.48

Table 7. Composition (wt. %) of the rotated Q-mode factors for Site 581 plotted in Figure 8.

Element	Factor 1	Factor 2	Factor 3
Ti	0.23	0.01	0.04
Al	5.15	15.0	0.00
Si	32.4	14.6	41.2
Mg	1.12	3.24	0.23
K	1.71	3.76	0.23
Ca	0.13	0.73	0.32
Ba	0.15	0.19	0.01
Mn	0.01	3.72	0.19
Fe	3.07	8.49	1.80
P	0.02	0.11	0.13

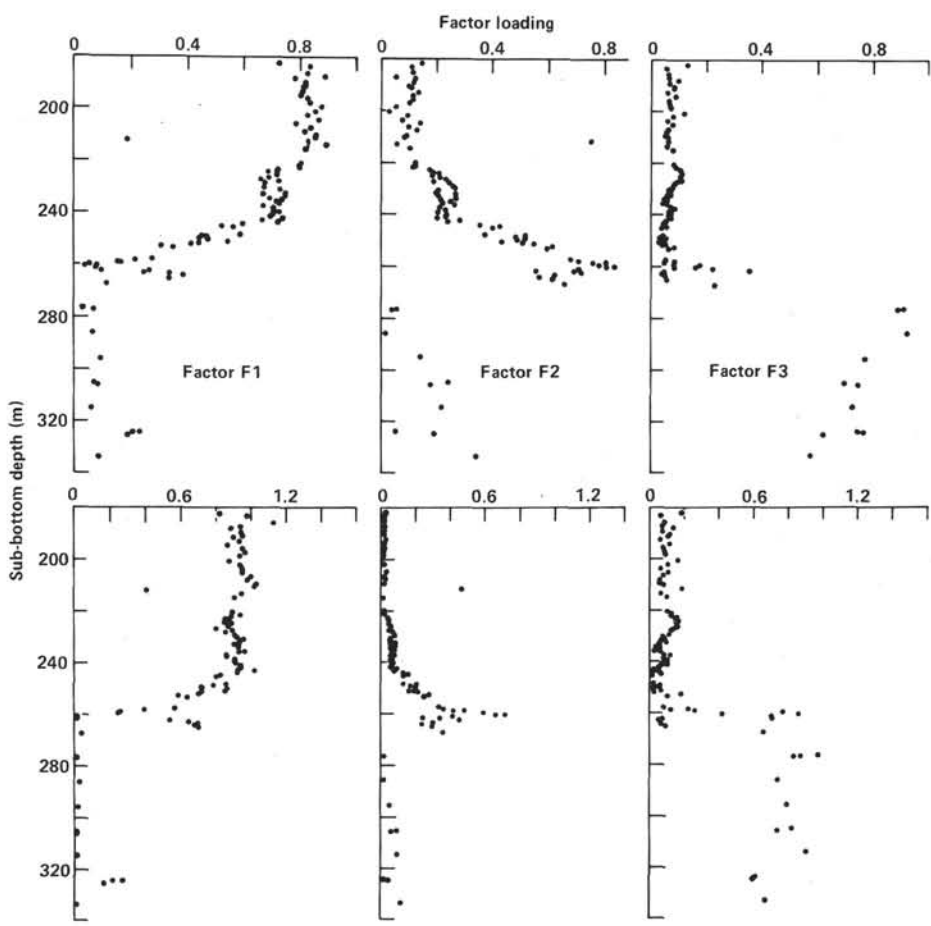


Figure 8. Downhole profiles of loadings of Q-mode varimax factors (upper), and rotated varimax factors (lower) on samples from Site 581. Elemental contributions to Q-mode factors are listed in Table 6. Compositions of rotated factors are listed in Table 7.